

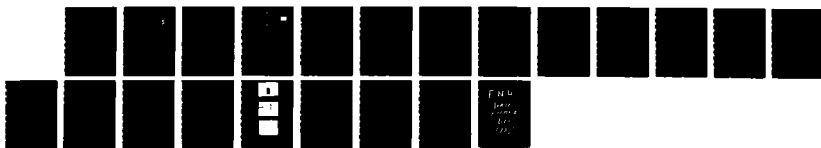
AD-A185 511

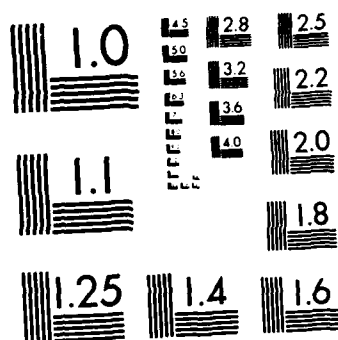
LOW-COST BISTABLE OPTICAL DEVICE FOR OPTICAL COMPUTING 1/1  
APPLICATIONS(U) OPTRON SYSTEMS INC BEDFORD MA  
C WARDE ET AL 1987 N00014-86-C-0806

UNCLASSIFIED

F/G 28/6

NL





MICROCOPY RESOLUTION TEST CHART  
NATIONAL BUREAU OF STANDARDS-1963-A

FINAL TECHNICAL ABSTRACT

12  
DTIC FILE COPY

Low-Cost Bistable Optical Device for Optical Computing Applications

Contract Number N00014-86-C-0806

AD-A185 511

Dr. Cardinal Warde  
Mr. Robert Dillon

Optron Systems, Inc.  
3 Preston Court  
Bedford, Ma 01730  
(617) 275-3100

DTIC  
ELECTE  
S OCT 08 1987 D  
CD

Optical computers and optically-implemented brain-like processors, known as neural networks, are recognized as potentially useful elements in the quest to meet the intense battle management requirements of the SDI program due. This is due to the inherently large degree of parallelism and interconnection capability of optical processors. Large, two-dimensional arrays of bistable devices with millions of pixels that exhibit intrinsic bistable or threshold-type switching characteristics are urgently needed to realize such optical processors. The low-cost bistable optical device discussed herein is ideal for the implementation and evaluation of several of the advanced algorithms and architectures proposed for optical computing. Its potential for high throughput, parallel addressing and readout, along with its optical gain and its low electrical and optical power consumption make it well suited for optical computing applications.

The Phase I effort explores a radically new approach for the development of a 2-D array of low-cost, high-resolution bistable optical elements. The proposed device is illustrated in Figs. 1a and 1b. Its bistable operation is based on electrical and optical coupling between thin layers of photoconductive and electroluminescent materials. This approach does not suffer from the stacking and scaling problems that plague semiconductor-based technologies and it leads to devices that consume little power, offer high sensitivity and are simple and inexpensive to manufacture. Consequently, this device can potentially be mass-manufactured at very low cost.

Such technology is expected to revolutionize multidimensional signal processing since truly parallel symbolic logic processing and "fuzzy" processing could be efficiently realized. Applications such as multispectral image processing, optical clutter rejection, target discrimination and identification, pattern recognition, industrial inspection, and other machine vision would also benefit from this technology.

DISTRIBUTION STATEMENT A  
Approved for public release  
Distribution Unlimited

87 9 16 009

## FINAL PHASE I TECHNICAL REPORT

### SUMMARY OF PHASE I WORK AND RESULTS

The Phase I effort conclusively demonstrated the feasibility of the low-cost bistable optical device (BOD) technology. After developing the required material processes to fabricate prototype devices, we fabricated a series of small-scale prototypes, evaluated their performance and optimized the fabrication procedure. The resulting prototypes contained approximately 2500 independent resolution elements in a  $2.25 \text{ cm}^2$  active area, operated with an optical gain of greater than 2.0, dissipated less than  $0.2 \text{ W/cm}^2$  of electrical power, switched at speeds greater than 1.0 Hz, latched images generated by a weak light emitting diode, operated in excess of twelve hours without suffering performance degradation, and required less than three dollars of raw materials to produce.

The Phase I effort was concentrated in the following four areas:

- 1) Device Modeling and Theory of Operation
- 2) Material Processing and Evaluation
- 3) Prototype Device Fabrication
- 4) Device Testing

A concise discussion of the results obtained from each effort follows.

#### Device Modeling and Theory of Operation

The crosssectional structure of the low-cost BOD is illustrated in Figure 1. The device consists of a photoconductive and an electroluminescent layer sandwiched between two transparent conducting electrodes and separated by an

Accession For	
NTIS CRA&I	<input checked="" type="checkbox"/>
DRIC TAB	<input type="checkbox"/>
Unannounced	<input type="checkbox"/>
Justification	
By <i>per th.</i>	
Distribution	
Availability Codes	
Dist	Avail and/or Special
A-1	

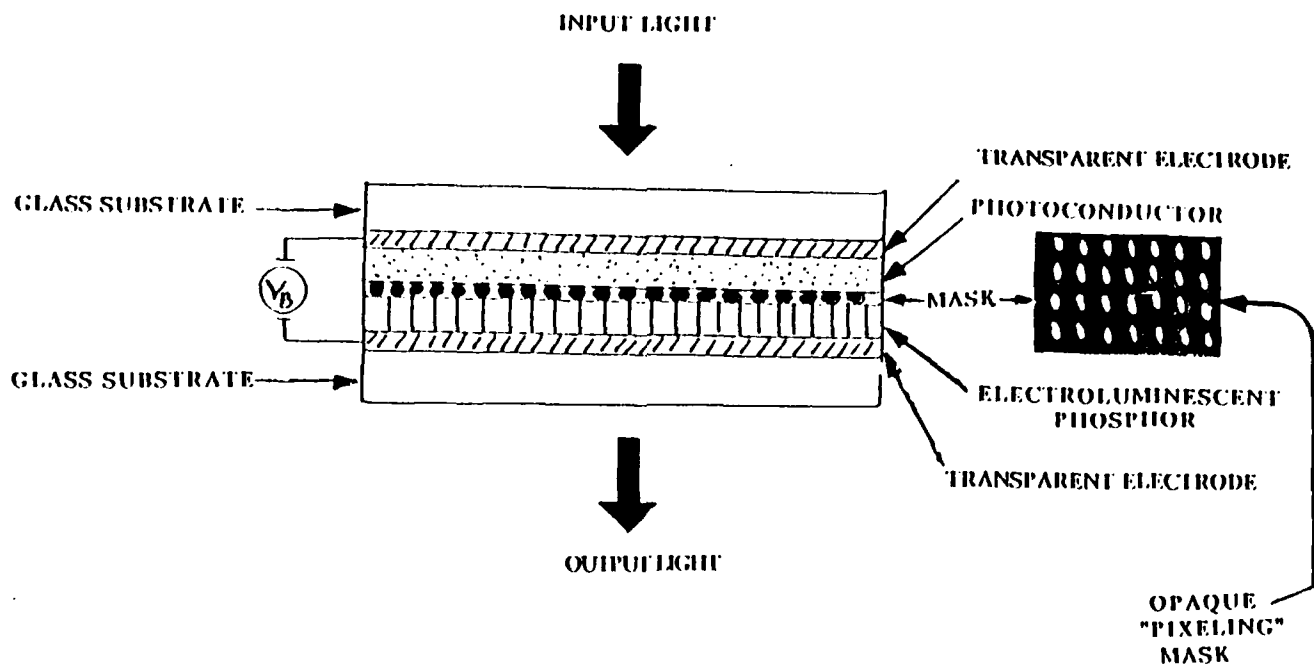


Figure 1 - Crosssectional Structure of the Low-cost Bistable Optical Device shown Schematically to Illustrate Multi-layer Design and Opaque "Pixelizing" Mask.

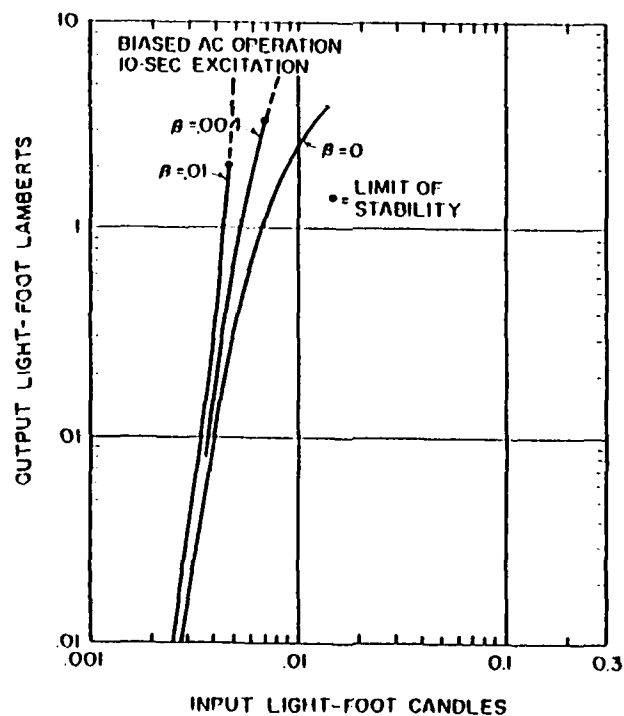


Figure 2 - Experimental Curves Showing Effect of Feedback on Input-Output Characteristic of Intensifier. (From B. Kazan, Proc. IRE 47, 12 (1959).

opaque, electrically insulating, pixeling mask. The "pixelized" mask is etched in a grid-like pattern to generate regions void of opaque material. The two transparent electrodes are driven by a direct voltage source,  $V_B$ , which provides the required longitudinal electric field through the layers. The device is then hermetically sealed to protect the electronic materials from atmospheric contaminants.

As input illumination is applied to the photoconductive layer, the resistance of the photoconductor decreases locally causing a greater percentage of the applied voltage ( $V_B$ ) to fall across the electroluminescent phosphor. When the external input illumination rises above some threshold level, the resulting increased field strength produces a glow in the phosphor, and since the emission from the phosphor is not shielded from the photoconductor at each pixel location, the glow lowers the resistance of the photoconductor even further. Eventually, this feedback process drives the pixel into the totally ON state. Further increases in the external illumination will not significantly increase the output emission because the phosphor voltage cannot rise above  $V_B$ . At this point the input light source can be removed and the activated pixels will remain "latched" in the ON state until the entire two-dimensional device is reset by momentarily removing the electrode bias voltage. The optical transfer function corresponding to this process is shown in Figure 2A.

Such a system was analyzed by Kazan in the late-1950's.<sup>1</sup> For a BOD with no internal optical feedback it can be shown that the output light intensity  $B_2$  is related to the input intensity  $B_1(t)$  by the expression

$$B_2 = A \left[ \int_0^t B_1(t) dt \right]^3 \quad (1)$$

where  $A$  is a constant.

If internal feedback is added, Eq. (1) becomes

$$B_2 = A \left[ \int_0^t (B_1 + \beta B_2) dt \right]^3 \quad (2)$$

where  $\beta$  is the fractional output intensity coupled back to the photoconductor.

Equation (2) applies only to the build-up of light at the BOD output. Empirical measurements have shown that the output intensity decay characteristics of an electroluminescent layer driven by a photoconductive layer is roughly exponential<sup>1,6</sup> and can therefore be expressed by

$$B_2 = B_p e^{-t/\tau} \quad (3)$$

where  $B_p$  is the output intensity at the moment decay begins and  $\tau$  is the system's decay time constant.

The output light intensity  $B'_2$  that exists when optical latching begins to occur can be derived from the combination of equations (2) and (3)<sup>2</sup> as

$$B'_2 = \frac{1}{A^{1/2} (\beta \tau)^{3/2}} \quad (4)$$

Kazan<sup>1</sup> experimentally determined the effect of varying the optical feedback strength,  $\beta$ , as it relates to both  $B'_2$  and the input-output transfer function of a BOD-like device. His results are shown in Figure 2.

Most electroluminescent phosphors exhibit a nonlinear transfer function relating input field strength to output light intensity as can be seen in Figure 3.<sup>3</sup> This feature allows the BOD to operate with a nonlinear threshold

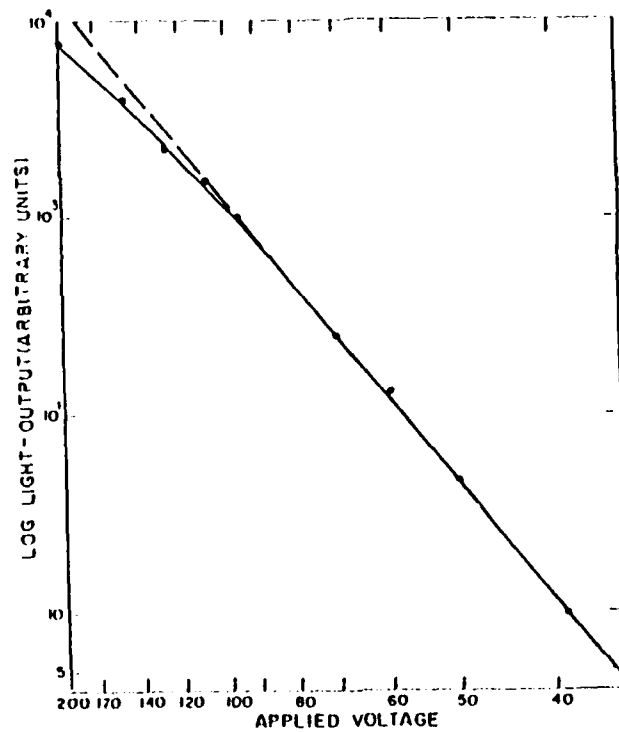


**Figure 3 -** Variation of Light Output with Applied Voltage for Conventional Electroluminescent Phosphors.

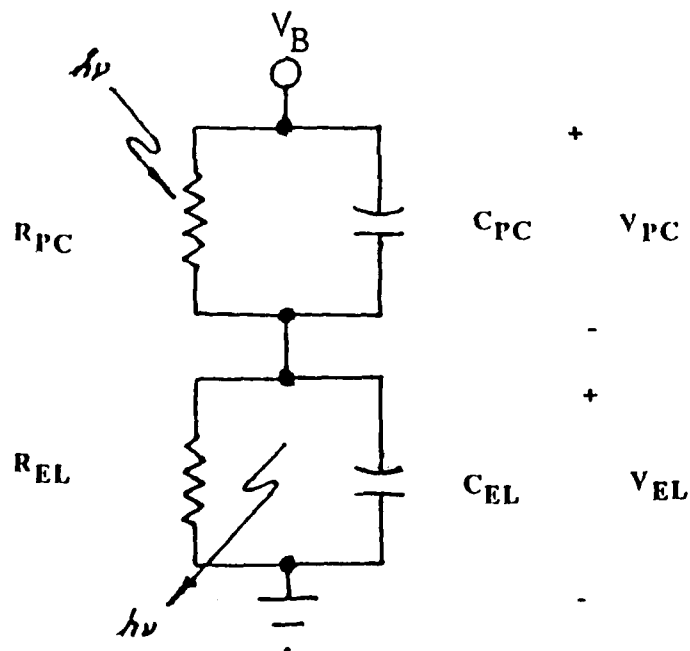


**Figure 4 -** Simple Circuit Model of a Single BOD Pixel.



and no latching when internal optical feedback is eliminated.

Figure 4 is an electrical model for one pixel of the device with  $V_B$  representing the bias voltage source,  $R_{PC}$  and  $C_{PC}$  representing the resistance and capacitance of the photoconductor and  $R_{EL}$  and  $C_{EL}$  representing the resistance and capacitance of the electroluminescent layer. Using a DC voltage source  $V_B$  with no external illumination on the photoconductor,  $C_{PC}$  and  $C_{EL}$  are essentially open circuits. In this case the bias voltage  $V_B$  divides resistively across  $R_{PC}$  and  $R_{EL}$  such that  $V_{PC} > V_{EL}$  if  $R_{PC}(\text{dark}) > R_{EL}$ . When  $V_B$  is set just below threshold,  $V_{EL}$  remains below the threshold required for the device to latch on. When sufficient input illumination impinges on the photoconductor,  $R_{PC}$  decreases resulting in an increase of  $V_{EL}$  and the generation of phosphor emission. If optical feedback is employed, the phosphor radiance will maintain a lowered  $R_{PC}$  value and latching will occur. A detailed electrical model and associated analysis for optically-coupled electroluminescent and photoconductor cells has been reported by Porada.<sup>4-5</sup>

#### Material Processing and Evaluation

The Phase I efforts were targeted at determining which material characteristics of the photoconductor and electroluminescent phosphor were essential for achieving high gain optically bistable arrays. It was found that maximum photoconductor responsivity and phosphor efficiency are necessary for achieving high switching speed in the device as well as low electrical power consumption. Particular attention was given to procedures for hermetic sealing of the device to impede moisture egress, which limits the lifetime of the phosphor. Additionally considerable effort was expended in Phase I developing the in-house capability to produce thick-film PC and EL layers.

The ultimate properties of an electroluminescent layer depend to a large extent on the nature of the phosphor employed and the fabrication techniques used in the deposition of the layer. Electroluminescent phosphors can be deposited in either "powder set" or thin-film forms. A powder set layer is made by screening or spraying a mixture of phosphor granules and organic binder onto a substrate whereas thin-films are deposited by vacuum evaporation. It has been shown<sup>6</sup> that powder set layers exhibit a considerably higher efficiency than thin-film layers. Thin-films, on the other hand, exhibit operational lifetimes of 40,000 hours relative to 1500 hours for thick-film systems. The powder set approach was chosen for the Phase I effort primarily because of the expense associated with thin-film deposition hardware.

The phosphor that was used exclusively during our Phase I investigation was zinc sulphide coactivated with copper and manganese.<sup>8-11</sup> While the Cu content controls the conductivity of the phosphor, recombination and light emission take place at the manganese luminescent centers. Manganese was chosen to serve as the luminescent center of the phosphor because of its yellow emission which has proved to be more efficient than the blues and greens.<sup>8</sup> The efficiency of the phosphor is further affected by both the concentration of the Mn and the Cu. The optimal amount of Mn has been shown to be .3 wt% while the amount of Cu should be .05 wt%. If bright panels were desired then the Cu content would need to be raised to .2 wt%.<sup>7</sup> A high chlorine content, which has been found in some commercially available phosphors, limits efficiency.

Several 5.0 cm<sup>2</sup> layers of EL were fabricated between glass slides containing transparent electrodes (ITO) during Phase I. Three suspending agents (binders) were tested to determine which would yield the best powder set matrix for the device performance. It was found that two of the three

binders tried severely degraded the lifetime and efficiency of the phosphor.

The first, cyanoethyl sucrose, proved the easiest to work with due to its availability and low toxicity. Cells produced with this binder exhibited a limited operational lifetime (~30 minutes), moderate switch-on voltages (200V), uniform emission across the 5.0 cm<sup>2</sup> sample, moderate output efficiency (relative to other binders tested), and suitable electrical properties (5MΩ/cm<sup>2</sup> at 400V). The limited lifetime of these cells forced us to pursue an alternate binder system.

The second binder investigated was polymethylmethacrylate (PMM). Our preparation methods were modified to coincide with that of Vecht.<sup>7</sup> PMM requires preparation in a solvent prior to use. The first three solvents tried were ethyl alcohol, xylene, and acetone. These provided unsatisfactory viscosities for application of the powder set to the ITO glass substrate. Toluene, however, proved satisfactory. Layers were then constructed using this solvent, polymethylmethacrylate and the ZnS(Mn:Cu) phosphor powder. These were then tested in the same manner as the earlier layers, with undesirable results. Specifically, even at large voltages (>600V) little to no light emission was measured.

Enormous success was achieved with the third proprietary binder. EL fabrication with this binder exhibited stable emission characteristics beyond 10 hrs and several days of shelf time. The output efficiency was far superior to that observed prior to its use. Also low switch-on voltages (~100V), uniform output emission over a 5.0 cm<sup>2</sup> area, and suitable electrical resistivities (~5MΩ/cm<sup>2</sup> at 400V) were common in devices fabricated with this compound as a binder. EL layers of this type were judged suitable for subsequent BOD feasibility tests.

The optical performance of the above-mentioned samples was monitored using

a Hamamatsu silicon detector followed by Tektronix AM 502 differential amplifier coupled to a Tektronix DM 501 Digital multimeter. Voltages were measured with a Keithley 132F voltmeter. Currents were monitored with a low-cost microammeter. A variety of phosphor/binder application techniques were tested including spin-on, spray-on, brush-on, screening and blade methods. Blade applications proved to be the method of choice due to the highly viscous nature of the slurry and the need for smooth, relatively thick and highly uniform layers.

Developing in-house capabilities to support the required photoconductor technology proved to be less strenuous relative to the effort required for EL phosphor production.

Much work has been reported in the literature regarding copper-activated cadmium sulphide (CdS) for use as a photoconductor and electrophotographic material.<sup>1 2 -1 4</sup> Like EL phosphor, CdS layers can be created in thick-film form using powder/binder sets or as thin films using vacuum evaporation techniques.

It has been shown that a dark-to-light resistance change of 167:1 can be achieved when CdS is mixed with a resin and applied as thick films.<sup>1 2</sup> As with EL phosphors, thick-films are far less costly to deposit than thin-films but are limited to switching times of about 0.8s. Thin-films are capable of 1.0 ms switching times.<sup>1 4</sup> As a matter of cost, we limited our Phase I BOD to the use of thick-film-based photoconductors. As a result, the prototype BODs exhibited optical switching times of about 1.0 Hz.

For the preparation of the PC layers, the method used by Faria and Karam<sup>1 2</sup> was employed. The layers were then characterized by measuring the dark and light resistances of the photoconductor at various voltages. The test set-up consisted of the CdS layer in series with an ammeter and a variable voltage supply. A 2-watt variable-intensity incandescent light source was placed

approximately 15 cm from the layer to provide controlled illumination. At varying illumination levels and operating voltages the photoconductor current was measured and the resistance calculated using Ohm's Law.

From this data it became apparent that the powder-to-binder ratio and the layer thickness are critical to achieving maximum sensitivity to incident light. When the optimum thickness and ratios were found we were able to observe resistivity changes greater than 70:1 at bias voltages as low as 100V. No absolute radiometric calibration was performed on the input illumination source used to produce the 70:1 resistivity changes in these samples.

### **Prototype Device Fabrication**

Three different device geometries were fabricated and tested to determine which configurations were appropriate to meet the Phase I goals. The first, referred to as the "discrete" design, consisted of individual EL and PC cells connected in series electrically and butt-coupled optically as shown in Figure 5. These devices, by design, were single-pixel versions of the BOD and were tested early in the Phase I effort to demonstrate the feasibility of optical switching. The second geometry, known as the "composite" design, utilized a mixture of EL phosphor and CdS photoconductor particles in a common binder slurry in an attempt to greatly simplify the structure of the device. The third design, called the integrated sandwich architecture, is illustrated in Figure 1A and consisted of discrete EL and photoconductor layers sandwiched between two ITO-coated glass substrates.

The earliest prototypes were of the discrete design. These contained phosphor cells that employed cyanoethyl sucrose as a binder and were observed to latch in a bistable manner when operated at 600-800V and illuminated at 15cm distance by a 2-watt incandescent source. From these early tests we

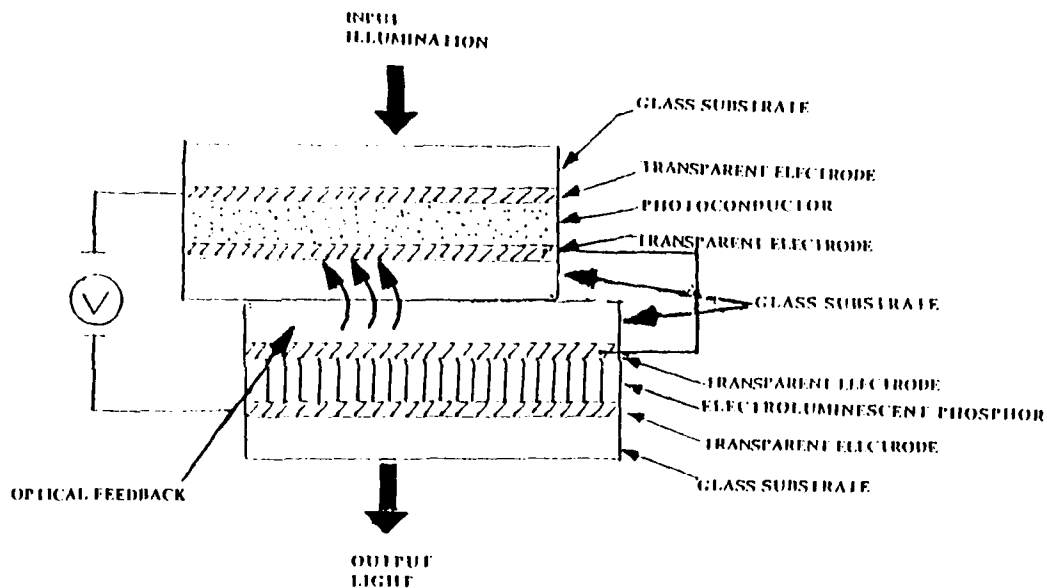


Figure 5 - "Discrete BOD Design Consisting of Totally Independent EL and PC Cells Used for Earliest Demonstration of "Single-Pixel" BOD Switching.

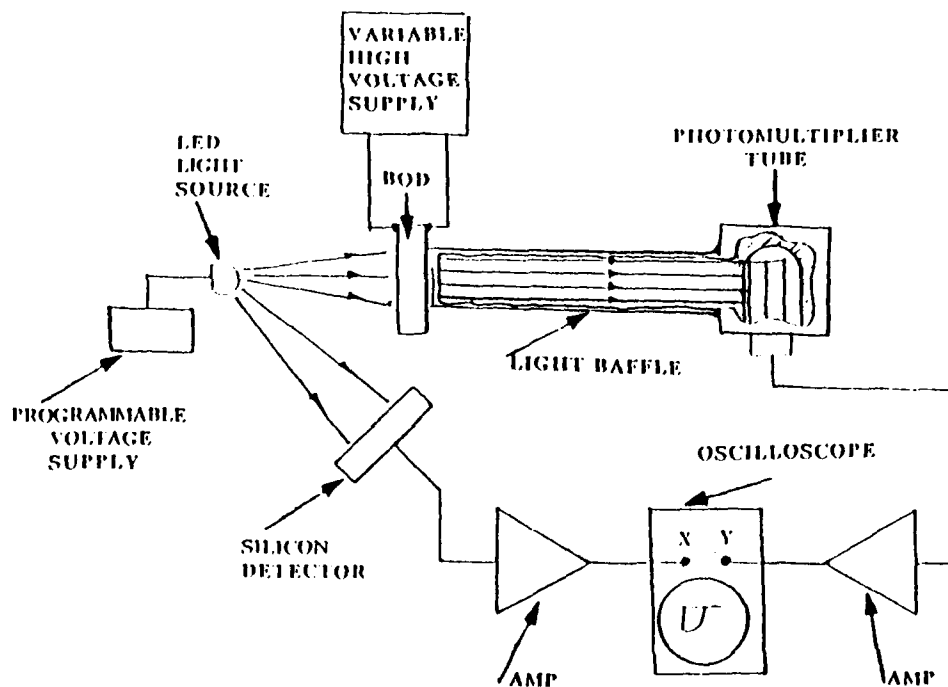


Figure 6 - Test Setup Used to Characterize the Gain, Threshold Voltage, Switching Speed and Input-Output Characteristics of Prototype Devices.

concluded that the PC and EL layers fabricated in-house were sufficiently sensitive and efficient to support bistable action.

Tests conducted with the composite architecture proved unsuccessful. A variety of photoconductor powder-to-phosphor powder ratios were tested as were several powder-to-binder ratios. In every case, no latching action was observed and very poor phosphor output efficiencies were noted. It was concluded that the composite structure holds little promise of working due to the incompatible requirements placed on photoconductor and phosphor binders. Specifically, the charge transport mechanisms required of the photoconductor binder are not well suited to the insulative properties and high dielectric constant needed in a good EL phosphor binder.

Two methods of "integrated sandwich" BOD construction were investigated and one method proved to be superior. In one approach, the phosphor layers were applied to an ITO coated substrate using the blade method. These layers were allowed to harden (cure) before a buffer layer was applied. Subsequent to buffer curing, a small amount of photoconductor/binder slurry was applied and a second ITO-coated substrate was pressed onto the slurry. The entire assembly was sealed with epoxy (around the perimeter) to prevent contamination.

Several devices were tested using a variety of buffer materials with varied results. In almost every case, the lifetimes of these "integrated sandwich" devices were greatly improved over those of the discrete devices.

Although these devices represented a considerable step forward in demonstrating BOD feasibility, it was observed that their output brightness was lower than previously-fabricated phosphor-only cells. It was also evident that the photoconductor/binder slurry produced a discoloration in the hardened phosphor layer irrespective of the buffer type employed. It was assumed that

the relatively volatile polymethylmethacrylate was penetrating through the thin buffer layer where it interacted with the phosphor to lower its efficiency.

To test this hypothesis, a second integrated sandwich geometry was developed that consisted of separately-cured PC and EL layers. This configuration is known as the separately cured integrated BOD. Individual, smooth layers of each material were applied to separate ITO-coated substrates and were mated together using a thin buffer layer. Special care was taken to seal these samples with epoxy immediately after fabrication to prevent moisture penetration and the resulting loss of phosphor efficiency.

The lifetime and output brightness of these BODs were far superior to those measured using any other fabrication technique, equaling those observed with individual PC and EL layers. For this reason, samples fabricated using the above-mentioned, separately-cured integrated sandwich approach were used exclusively in the tests described below.

#### Device Testing

Two prototype, 1.5 mm x 1.5 mm, pre-cured integrated sandwich bistable optical devices were fabricated to support a series of more quantitative performance tests. The first device was tested to determine its longevity, switching speed, gain and input-output characteristics using the test arrangement illustrated in Figure 6. Radiometric equipment was not available during the Phase I effort. For this reason absolute input irradiance levels were estimated based upon the expected radiance from a standard light emitting diode.

The prototype BOD was placed in the test setup and biased using the variable high voltage supply shown (See Figure 6). The device output



radiance was monitored using a highly sensitive Hamamatsu 95604 photomultiplier tube (PMT) and a preamplifier coupled to the y-axis amplifier in the oscilloscope. Input illumination was provided by a standard green light emitting diode (LED) positioned approximately 14 cm from the BOD. A silicon detector positioned near the LED recorded its relative output intensity. The silicon detector response was amplified and plotted on the X-axis of the oscilloscope. The output intensity of the BOD was recorded on the oscilloscope as a function of LED output intensity and BOD bias voltage. These data are presented in Figure 7 renormalized to show BOD input intensity scaled equally to BOD output intensity.

The data in Figure 7 reveal an optical gain of greater than 2.0 at 1000V bias. Optical latching is clearly present as is a variable input optical switching threshold which appears to depend heavily on device bias levels. The observed switching characteristics remained stable for the device under test over a period exceeding three days at which point testing was concluded.

The second, pre-cured integrated sandwich device was tested in the manner illustrated in Figure 8. A pulsed LED light source was used to momentarily illuminate a three-hole binary mask placed against the input face of the BOD. The BOD was biased just below threshold and the resulting BOD output image was recorded on film using the polaroid camera shown. Figure 9A contains a photograph of the binary, three hole mask used, Figure 9B shows the output face of the device at the moment the input illumination is pulsed on, and Figure 9C contains a photograph of the BOD output face approximately five seconds after the input light was removed. A clear, latched image of the input image is seen. Since this BOD did not contain a "pixelizing" mask between the PC and EL layers the output image slowly smeared laterally across the output of the device during a period of approximately 35-55 seconds.

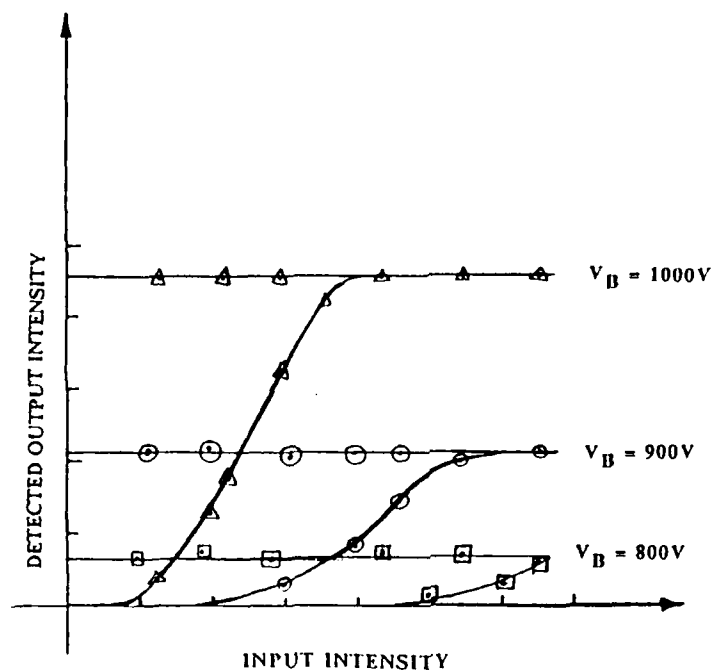


Figure 7 - Measured Input-output Characteristics for Phase I Prototype BOD Showing Bistable Latching and Variable Threshold for Indicated Bias Voltages (X and Y axes are scaled equally in intensity).

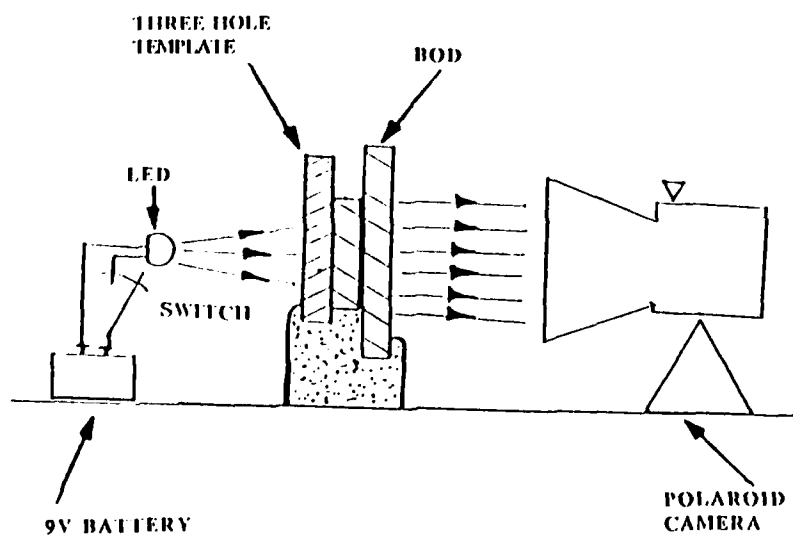
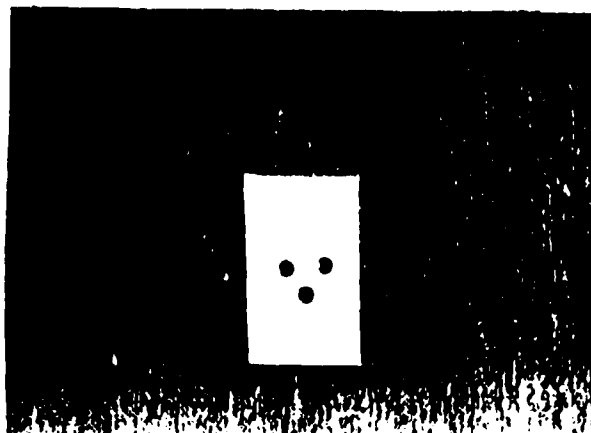


Figure 8 - Test Setup Used to Test the BODs Imaging Characteristics. The Pulsed LED Illuminates a Binary, Three-hole Mask Which is Proximity Focussed at the BOD's Input. The Device's Output Image is Recorded on Film Using the Polaroid Camera Shown.



**Figure 9A -** Photograph of Three-hole Binary Mask used for BOD imaging tests.



**Figure 9B -** Photograph of the BOD output face at the moment the input image is projected onto the rear face of the device.

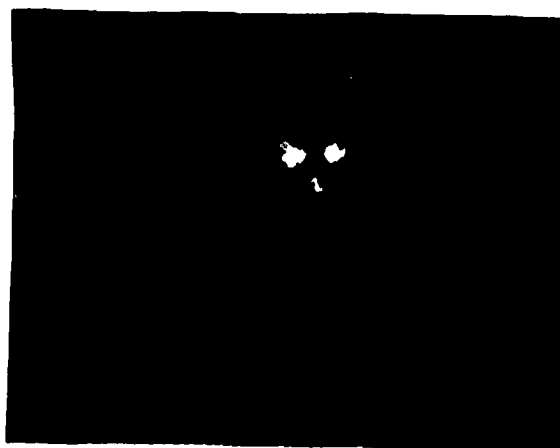


**Figure 9C -** Photograph of the BOD output face five seconds after the input image is removed. The latched image of the three-dot pattern is clearly visible.

Image erasure was achieved by momentarily interrupting the bias to the device.

In conclusion, the Phase I effort clearly demonstrated the feasibility of this technology. Furthermore, it provides a sound experience base upon which a successful Phase II development effort has been designed to extend the performance and manufacturability of this class of devices.

#### REFERENCES

1. B. Kazan, "A Feedback Light-Amplifier Panel for Picture Storage," Proc. IRE, 12 (1959).
2. F. H. Nicoll, "Solid State Image Intensifiers," in Photoelectronic Materials and Devices, Simon Larach, Editor, Van Nostrand, Princeton (1965).
3. A. G. Fischer, et. al, "Luminescence of Solids," in Photoelectronic Materials and Devices, Edited by S. Larach, Nostrand, Princeton, 17 (1965).
4. Z. Porada, "Thin Film Light Amplifier with Optical Feedback," Thin Solid Films, 109, 213 (1983).
5. Z. Porada, "Thin Film Light Amplifier," Thin Solid Films, 71, 209 (1980).

2. T. Williams, "Optics and Neural Nets: Trying to Model the Human Brain," *Computer Design*, 47 (March 1987).
7. A. Vetch, N. J. Werring, R. Ellis, and P. J. F. Smith, "Materials Control and D. C. Electroluminescence in ZnS:Mn, Cu, Cl Powder Phosphors," *Brit. J. Appl. Physics (J. Phys. D)*, 2, 953 (1969).
8. A. Vetch, N. J. Werring, R. Ellis, and P. J. F. Smith, "Direct-Current Electroluminescence in Zinc Sulphide: State of the Art," *Proc. IEEE*, 61, 902 (1973).
9. A. Vetch, N. J. Werring, and P. J. F. Smith, "High-efficiency D. C. Electroluminescence in ZnS (Mn, Cu)," *Brit. J. Appl. Phys. (J. Phys. D)*, 1, 134 (1968).
10. E. Schlam, "Electroluminescent Phosphors," *Proc IEEE*, 61, 894 (1973).
11. H. Kwarada and N. Ohshima, "DC EL Materials and Techniques for Flat-panel TV Display," *Proc. IEEE*, 61, 907 (1973).
12. S. Faria and R. Karam, "Electrical Properties and Imaging Characteristics of CdS: Cu, Cl in the Xerographic Mode," *J. Appl. Photog. Eng.*, 7, 102 (1981).
13. Z. Porada, "Influence of the Aging Process on the Photoconductivity

Properties of CdS (Cu, Cl) Thin Films," Thin Solid Films, 110, 1 (1983).

14. Z. Porada, "Photoconductivity Growth and Decay Time of CdS (Cu, Cl) Films," Thin Solid Films, 66, L55 (1980).

END

DATE  
FILMED

DEC.

1987